Assessment of Iron Oxide Nanoparticle Concentration for Distinct Intercranial EEG Electrode Localization in MRI

Johannes B. Erhardt[1,2], Jessica A. Martinez[2], Tyler E Cork[2], Isabel Gessner[3], Sanjay Mathur[3], Thomas Stieglitz[1], and Daniel B. Ennis[2]

[1]*University of Freiburg, Freiburg, Germany,* [2]*UCLA, Los Angeles, CA, United States,* [3]*University of Cologne, Cologne, Germany*

Synopsis

IcEEG electrodes for epilepsy and research applications impair fMRI and MR images with compromising susceptibility artifacts. Thin-film implants feature 100x less metal thickness and thus minimal artifacts. However, thin-film implants are inconspicuous in MRI. Therefore we present means of localization using super paramagnetic iron oxide nano particles to make thin-film implants ready for future applications. We present feasible concentrations and proof of concept.

Introduction

Intercranial EEG (icEEG) electrodes are implanted for pre-surgical assessment of cortical electrical activity in patients with epilepsy. MRI helps to localize the implant with respect to the individual's anatomy and fMRI can improve understanding of the neuropathology. However, the magnetic susceptibility artifacts caused by the metal components of commercially available implants produce MRI artifacts that compromise the results especially in the direct vicinity of the implants. Next generation "thin-film" implants which feature 100x less metal thickness can mitigate these artifacts, but thin-film implants produce inconspicuous MRI signal voids in many clinical MRI sequences. Imperatively, physicians need to know the implant position and the value of EEG increases with the precision of electrode localization. Therefore, we investigated various concentrations of super paramagnetic iron oxide (SPIO) nanoparticles (NP) to label thin-film implants for localization in MRI using a range of sequences. In particular, we aim to create a marker that conspicuously renders the implant, enables spatial localization of the individual electrodes, and keeps disruptive imaging artifacts small.

Materials and Methods

Eight samples of silicone rubber doped with various SPIO-NP concentration were fabricated. SPIO-NPs were synthesized using oleic acid as surface active ligand to obtain SPIO-NPs which were soluble in n-heptane [1]. The SPIO-NPs were then added to n-heptane and mixed with MED1000 silicone rubber (Nusil). The mixture was spin coated on substrates to achieve homogenous layer thickness where the thicknesses vary among samples. By weighing the samples with a precision scale, dividing their weight by their length and multiplying by SPIO-NP concentration in weight% we obtained a measure of the amount of NPs per cross-section in arbitrary units termed "concentration" in the following (Table1).

A strip of each sample was arranged on a polyimide sheet (Figure1), then embedded in 1% agarose gel to mimic MRI contrast of gray matter [2,3]. The polyimide sheet was then placed in a 3T scanner (Siemens Skyra) and imaged using a T2 TSE STIR sequence as commonly used in clinical post-implantation practice [4] employing a body coil and the vendor's standard epilepsy protocol with a transmit/receive head coil. From the acquired sagittal T2 TSE STIR sequence images, we extracted a signal intensity profile as shown in Figure1. A deviation of 30% from the background signal intensity (ASTM2119) was used to define and calculate the artifact area of each sample (Figure2, Table1). We then took two 128 channel thin-film icEEG implants made of 300 nm thick platinum iridium sandwiched in a layer of 5µm polyimide on either side (fabrication: [5]) using sample #7 as marker on one of the implants (Figure3). Then both implants were embedded in 1% agarose using the same MRI protocol as before with the implants in the axial orientation as intended for use.

Results

Figure1 shows that sample #1, #2, #4, and #5 exhibit limited artifacts according to ASTM2119. The artifact created by sample #8 exceeds the sample dimensions. Samples #3, #6 and #7 show distinct image artifacts without exceeding their sample dimensions excessively. Figure2 suggests a correlation between the "concentration" of SPIO-NPs and the imaging artifact size. Figure3 illustrates the application of sample #7 as thin-film icEEG implant marker for localization in MRI. All MR images show that the implants themselves appear with little to no contrast compared to the gel background. The SPIO-NP marker creates contrast that facilitates localization of the implant and can be used as a reference to locate the individual electrodes. Notably, the SWI image displays single electrodes.

Discussion

The "concentration" of samples #4 and #5 are close to the artifact threshold and therefore resemble minimum "concentration". Sample #3, #6 and #7 show artifacts and the artifact size remains close to the sample dimensions and therefore fulfills our requirements of marking the implant while keeping the disruption of the image small. Sample #8 shows 5x artifact size of #7 which results in excessive concealment which is counterproductive. Figure3 shows good results for identifying the thin-film implant location with SPIO-NPs in the GRE sequence while the TSE sequences allow for unimpaired observation of the surroundings. In the SWI sequence the SPIO-NP markers provide conspicuous localization of the location of the implant. The illustration of single electrode sites may be of great value for electrode registration in brain function mapping. Further work is needed to evaluate the electrode conspicuity when the electrode is surrounded by tissue and placed on a curvature such as the brain. For a better correlation between the SPIO-NP concentration and the resulting imaging artifact size a wider range of SPIO-NP "concentration" should be investigated.

Conclusion

We show examples of SPIO-NP concentration that allow conspicuous localization of thin-film icEEG implants in MRI and localization of single electrode sites while keeping disruptive artifacts small.

Acknowledgements

The icEEG implants were generously made available by Christian Bentler. Partially funded within "BrainLinks-BrainTools" by the German Research Foundation (DFG ExC1086).

References

[1] Park, J., An, K., Hwang, Y., Park, J. G., Noh, H. J., Kim, J. Y., ... & Hyeon, T. (2004). Ultra-large-scale syntheses of monodisperse nanocrystals. Nature materials, 3(12), 891-895.

[2] Mitchell, M. D., Kundel, H. L., Axel, L., & Joseph, P. M. (1986). Agarose as a tissue equivalent phantom material for NMR imaging. Magnetic resonance imaging, 4(3), 263-266.

[3] Hellerbach, A., Schuster, V., Jansen, A., & Sommer, J. (2013). MRI phantoms–are there alternatives to agar? PloS one, 8(8), e70343.

[4] Jiltsova, E., Möttönen, T., Fahlström, M., Haapasalo, J., Tähtinen, T., Peltola, J., ... & Lehtimäki, K. (2016). Imaging of anterior nucleus of thalamus using 1.5 T MRI for deep brain stimulation targeting in refractory epilepsy. Neuromodulation: Technology at the Neural Interface, 19(8), 812-817.

[5] Boretius, T., Badia, J., Pascual-Font, A., Schuettler, M., Navarro, X., Yoshida, K., & Stieglitz, T. (2010). A transverse intrafascicular multichannel electrode (TIME) to interface with the peripheral nerve. Biosensors and Bioelectronics, 26(1), 62-69.

Figures

Sample #	1	2	3	4	5	6	7	8
NP Concentration in Weight%	0.000	0.033	0.066	0.100	0.132	0.200	0.300	0.600
Weight in mg	3.9	4.6	8.2	2.7	1.2	10	5.9	13.4
Length in mm	20.5	20.2	20.9	20.5	20.8	21.5	21.4	21.3
"Concentration" in A.U.	0.0000	0.0060	0.0241	0.0137	0.0085	0.0980	0.0786	0.3652
Artifact Size in mm²	0.0000	0.0000	1.2238	0.0000	0.0000	2.1416	3.0595	15.9093

Table 1 SPIO-NP doped silicone sample properties and resulting imaging artifact size for 30% threshold.

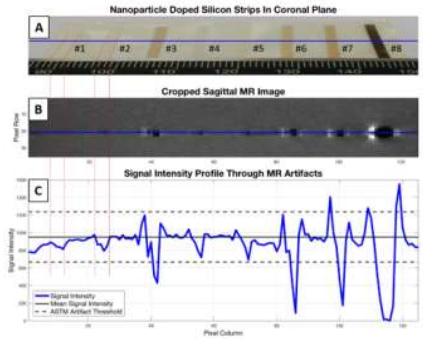

Figure 1. (A) Evaluation of MRI artifacts caused by SPIO-NP doped silicone strips for a range of SPIO-NP concentrations and sample thicknesses. The top photograph shows the eight sample strips arranged on 5µm polyimide substrate. Sample #1 has no incorporated SPIO-NPs while #8 appears dark due to the 0.6w% SPIO-NPs. The blue line indicates the approximate intersection of the MR image. **(B)** Resulting T2 TSE STIR MR image at 3T (Siemens, Skyra). The blue line corresponds to the signal intensity profile shown in **(C)** wherein the ASTM artifact threshold is also identified to define a cut-off concentration for SPIO-NP conspicuity.

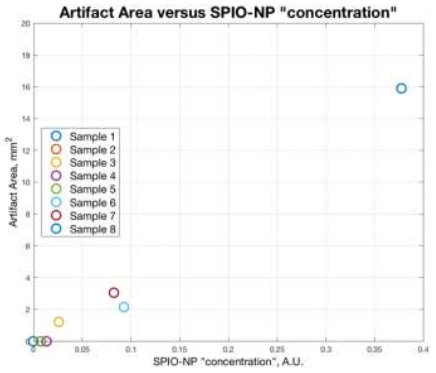

Figure 2. Plot of the artifact area above the 30% threshold in mm2 versus the SPIO-NP “concentration”. One should note that the threshold of 30% signal intensity change reduces the artifact area of four samples to zero and are therewith excluded from the correlation.

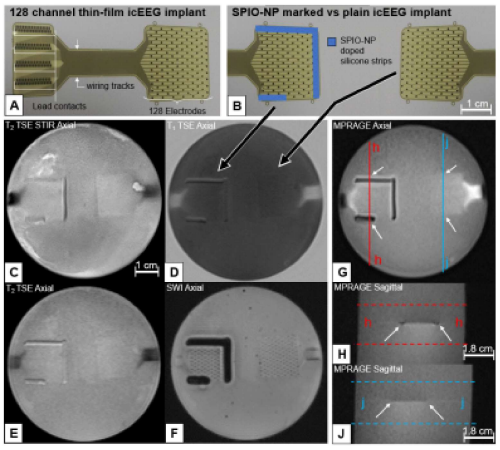

Figure 3. (A) Photograph of icEEG implant. **(B)** Phantom arrangement of two icEEG implants in clinically relevant position; the left one has SPIO-NP markers. For image artifact testing the wiring tracks and lead contacts were directed into the sagittal plane as if externalized. **(C-E)** T2w TSE STIR, T1w TSE, T2w TSE sequences in the axial view, respectively. **(F)** SWI sequence in an axial view illustrating location of single electrode sites and SPIO-NP markers clearly. **(G)** T1w GRE in the axial view. **(H, J)**: T1w GRE in the sagittal view as indicated in G.